Journal of Ceramic Processing Research. Vol. 10, No. 6, pp. 803~806 (2009)

J O U R N A L O F
Ceramic Processing Research

Structural and pyroelectric properties of $YBa_2Cu_3O_{6+x}$ for the uncooled infrared detectors

Sung-Pill Nam, Hyun-Ji Noh and Sung-Gap Lee*

Dept. of Ceramic Engineering, Eng. Res. Insti., Gyeongsang National University, JinJu-Si, Korea

The uncooled pyroelectric infrared based on semiconductor $YBa_2Cu_3O_{6+x}$ (YBCO) have been investigated. YBCO powder was prepared by a mixed oxide method and YBCO thick films were fabricated by the screen-printing method. The YBCO thick films were sintered at 820-945 °C. As a result of the Thermogravimetry and differential thermal analysis (TG-DTA), endothermic peak was observed at around 800 °C due to the formation of the tetragonal phase. YBCO thick films showed the typical XRD patterns of tetragonal phase and second phase was observed. The average particle size of YBCO thick films was about 1.67 μm. The thickness of the YBCO thick films was about 60 μm. The temperature coefficient of resistance (TCR = 1/R* dR/dT) of 930 °C-20min sintered YBCO thick films was −2.3% and the pyroelectric coefficient was 511.1×10^{-7} C/cm^{2}K.

Key words: YBCO, Thick films, Screen-printing, Pyroelectric, TCR.

Introduction

Recently, $YBa_2Cu_3O_{6+x}$ (YBCO) has been investigated as an uncooled microbolometer and pyroelectric detectors. $YBa_2Cu_3O_{6+x}$ are best known as a high temperature superconductor. The optical and electronic properties of $YBa_2Cu_3O_{6+x}$ are determind by its oxygen stoichimetry [1, 2]. For x 1, YBCO possesses an orthorhombic crystal structure, exhibits metallic conductivity, and becomes superconductive upon cooling below its critical temperature [3]. As x is decreased to 0.5, the crystal undergoes a phase transition to a tetragonal structure and it exhibits semiconducting conductivity characteristics as it exists in a Fermi glass state. As x is decreased further below 0.3, YBCO becomes a Hubbard insulator with a well defined energy gap on the order of 1.5 eV.

Recently, many piezoelectric applications, such as sensors and micro pumps, require ferroelectric ceramics with a thickness of less than 100 μm. There are some reports on fabrication of PZT thick films by sol-gel method, screen printing method, sputtering method and hydrothermal synthesis method [4, 5]. The screen printing method is especially useful for a high productivity and good cost performance brings the films to the stage of commercial mass production [6].

In this paper, YBCO thick films were prepared by the screen-printing method in order to decrease to improve the structural and pyroelectic properties. The structural and the pyroelectric properties as functions of the sintering condition, was investigated for pyroelectric applications.

*Corresponding author:
Tel : +82-55-751-5333
Fax: +82-55-758-1987
E-mail: lsgap@gnu.ac.kr

Experiments

The chemical compositions of the samples were given according to the following formula: $YBa_2Cu_3O_{6+x}$. This $YBa_2Cu_3O_{6+x}$ (YBCO) composition gave a transition temperature near the ambient room temperature. YBCO powders, started with a mixture of Y_2O_3, $BaCO_3$, and CuO, were prepared by the mixed-oxide method. The powder was dried slowly at 100 °C for 72 h and then calcined at 820 °C for 24 h in a high-purity alumina crucible. The screen-printable pastes were prepared by kneading the ground YBCO powder with 25 wt% of organic vehicle (Ferro. 75001). High purity alumina and yttria-stabilize-zirconia (YSZ) was used as a substrate. Al_2O_3 substrate reacted with YBCO and used YSZ at the higher temperature of Ts = 920 °C [7].

.The bottom electrodes were prepared by screen printing method Pt paste and firing at 1400 °C for 2 h. After screen printing, the YBCO paste using a 200 mesh screen mask, printed films were allowed to level for 10 min and then dried at 80 °C for 30 min. These processes of printing and drying were repeated 4-times to obtain a desired thickness. The coated thick films were sintered at 825-945 °C for 10-60 min in the closed alumina crucible. Substrate and sintering condition are shown in Table 1.

Table 1. Substrate and sintering condition of YBCO thick films

		Sintering temperature						
		825 °C	850 °C	875 °C	900 °C	915 °C	930 °C	945 °C
Substrate		Al_2O_3			YSZ			
Time	10min				O	O	O	O
	20min				O	O	O	X
	60min	O	O	O				

The thermal decomposition of the sols, dried at 100 °C, was followed by simultaneous thermal analysis thermogravimetry and differential thermal analysis (TA, SDT Q600, USA). Particle size distribution of calcined YBCO was measured by particle size analyzer (Sympatec, RODOS, Germany). The crystalline phase was identified by an X-ray diffractometry (Bruker, AXS D8 DISCOVER with GADDS, Germany). The surface and cross-sectional microstructure was examined by a field emitting scanning electron microscope (Philips, XL30 S FEG, Netherland). For the electrode formation, fired-on silver paste was used on both surfaces of the specimens. The dielectric properties of the specimens were measured suing LCR-meter (Fluke, PM6306, Germany). Relative resistance and dielectric loss as function of temperature were measured using LCR meter and thermostatic chamber (Delta design, Delta 9023, USA).

Results and Discussion

Fig. 1 shows Particle size distribution of the YBCO powder at calcinied with 820 °C. It can be seen that the particle size distribution of the YBCO powder derived from the mixed oxide process is uniform with the mean particle size of about 1.69 m. The distributions range of YBCO powder was 0.2-15 m.

Fig. 2 shows TG-DTA curve of dried YBCO powder at 100 °C of 72 h. The observation of a small endothermic peak below 250 °C was due to loss of chemically bonded water or dissociation of hydroxides. From the TG-DTA plots it was also evident that the formation of YBCO started at 800 °C.

Fig. 3 shows X-ray diffraction pattern of YBCO thick films with the variation of sintering temperature and time. All YBCO thick films showed the typical XRD patterns of tetragonal phase and second phase was observed. But second phase decreased with increasing the sintering temperature and time. It can be understood in terms of

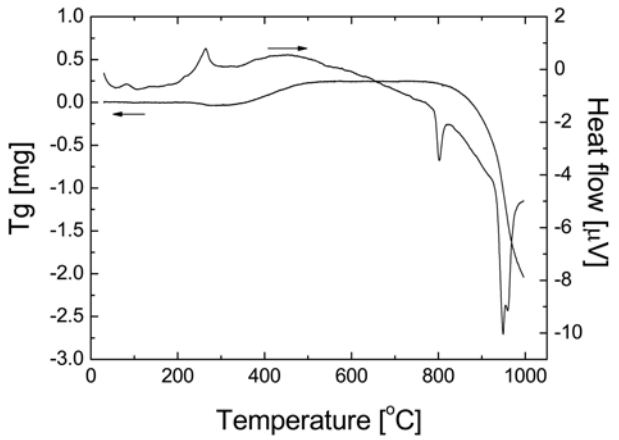

Fig. 2. TG-DTA curve of dried YBCO powder at 100 °C of 72 h.

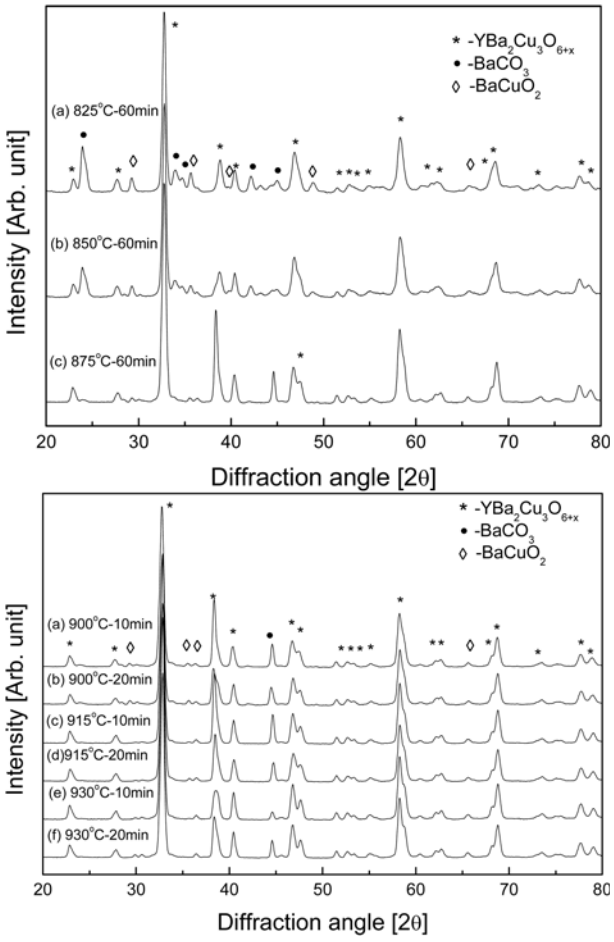

Fig. 3. X-ray diffraction pattern of YBCO thick films with the variation of sintering temperature and time.

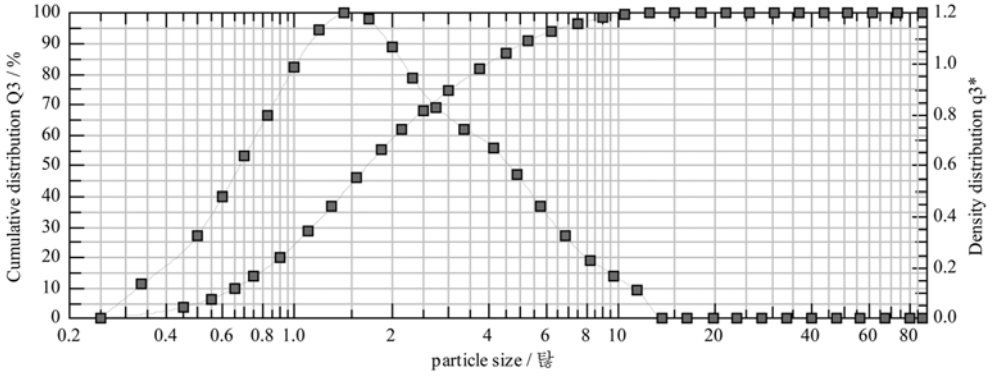

Fig. 1. Particle size distribution of calcined YBCO powder.

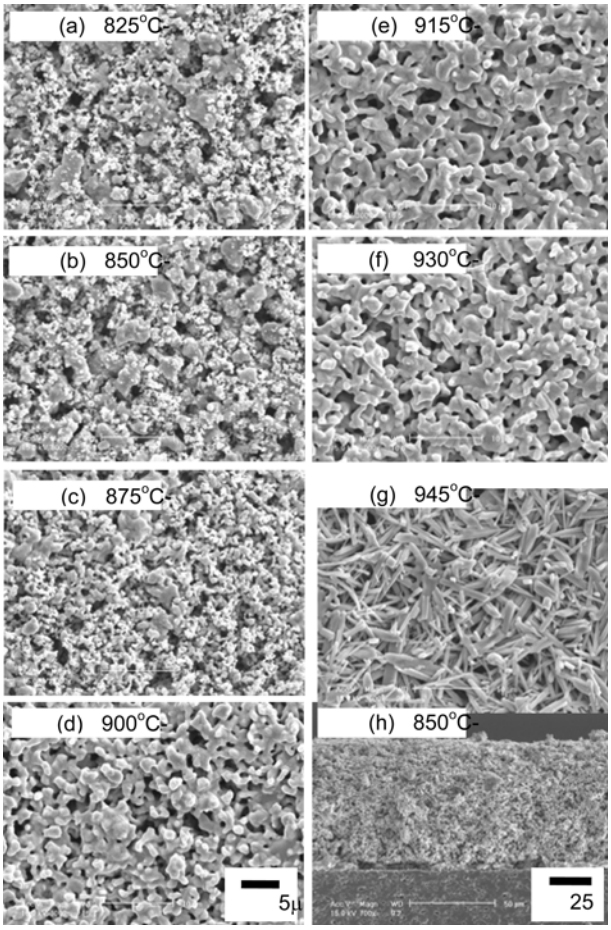

Fig. 4. Surface and cross-sectional SEM micrographs of YBCO thick films with the variation of sintering condition.

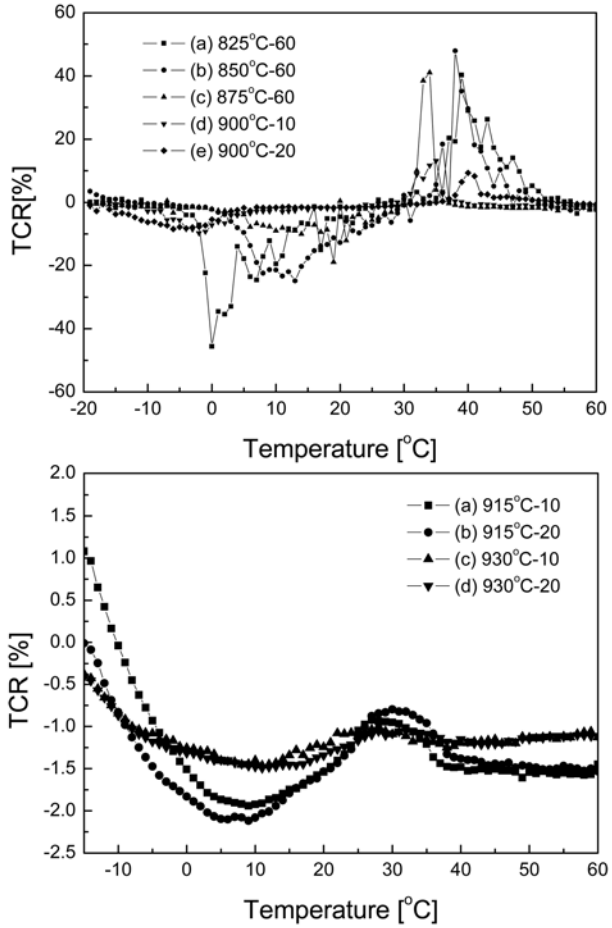

Fig. 5. Temperature Coefficient of Resistance (TCR) of the YBCO thick films with the variation of sintering condition.

the effect of the increment of disassembly of $BaCO_3$ and $BaCuO_2$.

Fig. 4 shows the surface and cross-sectional SEM micrographs of the YBCO thick films with the variation of sintering temperature and time. The surface micrograph of sintered YBCO thick films at 825 °C, 850 °C and 875 °C were a porous structure and consisted of mixed $YBa_2Cu_3O_{6+x}$ phase and second phase. And the densification of the YBCO thick films increased with increasing the sintering temperature. But surface micrograph of sintered YBCO thick films at 945 °C shows needle phase. The average thickness of thick films was about 60-65 m.

Fig. 5 shows the Temperature Coefficient of Resistance (TCR) of the YBCO thick films with the variation of sintering temperature condition. The TCR of sintered YBCO thick films at less than 900 °C changed greatly. These properties can be understood in terms of the effect of the component with unstable YBCO phase and second phase. But the TCR of sintered YBCO thick films at more than 900 °C changed smoothly. This is because second phase was reduced to high temperature. The TCR of sintered YBCO thick films at 915 °C of 20 min was -2.3%.

Fig. 6 shows the relative dielectric constant of the YBCO thick films with the variation of temperature. The Curie

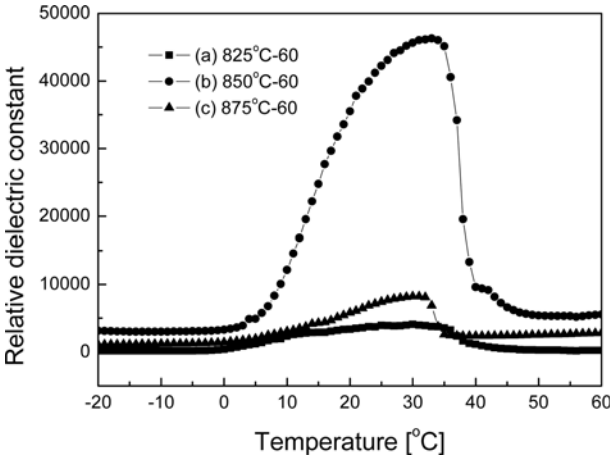

Fig. 6. Relative dielectric constant of the YBCO thick films with the variation of temperature.

temperature of the YBCO specimen sintered with 850 °C was 33 °C, and the dielectric constant was 51484.

Fig. 7 shows the pyroelectric coefficient of the YBCO thick films with the variation of temperature. The YBCO specimen sintered with 875 °C -60 min showed the maximum value of 511.1×10^{-7} C/cm^{2}K at Curie temperature in spite of their second phase because the specimen

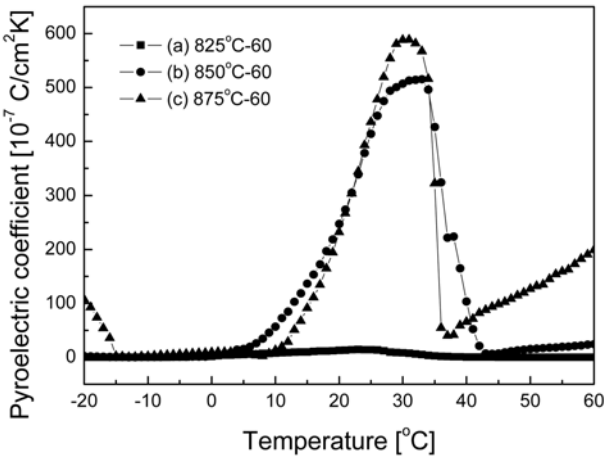

Fig. 7. Pyroelectric coefficient of the YBCO thick films with the variation of temperature.

have the high dielectric constant and the large variation of the dielectric constant-temperature curve.

Conclusion

In this research, YBCO thick film fabricated by screen-printing method. The YBCO thick films were annealed at 820-945 °C. The average particle size of YBCO calcined with 820 °C for 24 h was about 1.69 m. All YBCO thick films showed the typical XRD patterns of tetragonal phase and second phase was observed. The densification of the YBCO thick films increased with increasing the sintering temperature. The average thickness of YBCO thick films was about 60-65 m. The TCR of sintered YBCO thick films at 915 °C of 20 min was –2.3%. The Curie temperature of the YBCO specimen sintered with 850 °C was 33°C, and the dielectric constant was 51484. The YBCO specimen sintered with 875 °C -60 min showed the maximum value of 511.1×10^{-7} C/cm^{2}K at Curie temperature.

Acknowledgment

This work has been supported by ESRI (R-2005-7-094), which is funded by MOCIE (Ministry of Commerce, Industry and Energy).

References

1. I. Poberaj and D. Michailovic, ferroelectrics, 128 (1992) 197-199.
2. A. Jahanzeb, C.M. Travers, D.P. Butler, Z. Celik-Kutler and J. E. Gray, Appl. Phys. Lett., 70 (1997) 3495-3498.
3. G. Yu and A. Heeger, Int. J. Mod. Phys. Rev., B 48, 16 (1993) 6492-6498.
4. Y. Ohba, M. Miyauchi and M. Adachi: Jpn. J. Appl. Phys. 32 (1993) 4095-4098.
5. M. Okuyama and Y. Ishibashi: Ferroelectric Thin Films, Topic Appl. Phys., 98 (2005) 21-25.
6. V. Walter, P. Delobelle, P.L. Mlal, E. Joseph and M. Collet, Sensors and Actuators A, 96 (2002) 157-166.
7. T. Cheung and E. Ruckenstein, J. Mater. Res., 4 (1989) 1860-1870.